CFD-BASED AERODYNAMIC SHAPE OPTIMIZATION FOR JAPANESE EXPERIMENTAL SUPERSONIC TRANSPORT

Zhong Lei, Yoshikazu Makino
Advanced Aircraft Technology Center, Japan Aerospace Exploration Agency
7-44-1 Jindaiji-higashi, Chofu, Tokyo 182-8522, Japan

Keywords: *Supersonic Transport, Aircraft Design, Shape Optimization, Aerodynamics, Computational Fluid Dynamics*

Abstract

In order to establish advanced technologies for the next generation supersonic civil transport, Institute of Space Technology and Aeronautics of Japan Aerospace Exploration Agency has been promoting a scaled supersonic experimental airplane program, namely NEXST (National EXperimental Supersonic Transport), since 1997. To improve aerodynamic performance and reduce the cost of design process, an aerodynamic design tool, which combines a three-dimensional Euler CFD code with a gradient-based optimization technique, is developed. A multi-block/overset grid technique is utilized in the CFD analysis to simulate the flow-field around complex configuration of the airplane. A continuous adjoint sensitivity analysis is used for reducing computational cost in each design cycle of the optimization process. The paper describes optimization design technologies and some applications of CFD-based aerodynamic shape optimization conducted for a jet-powered supersonic experimental airplane in the program.

1 Introduction

The aircraft design has traditionally been based on empirical methods and linear theories, and supported by extensive wind tunnel testing to refine shape and flight testing for validation. Wind tunnel testing is capable to determine performance of scaled models, but it is limited by scale effect and can not avoid support and wall interference. The linear design methods predict the aerodynamic performance efficiently, and are very useful in the preliminary design phase. However, the linear method is restricted to problems that the flow around an aircraft is steady, unseparated, and does not contain any strong vortices and shock waves. Generally, it has low order in accuracy to estimate the aerodynamic performance. With the development of computer and numerical algorithms, computational fluid dynamics (CFD) has been widely accepted as an important role for aircraft design to shorten the overall design process and reduce cost. Although CFD has not such limitations of wind tunnel testing, the use of CFD in the design is strongly dependent on the computer power and the computing accuracy.

Aerodynamics of aircraft is complicated by many critical phenomena, such as shock wave, boundary layer, separation, component interference and so on. It is necessary to estimate aerodynamic performance accurately and capture important phenomena correctly in design process. Moreover, an essential requirement for aircraft design is the capability to treat complex geometric configurations because interference effect of component integration should be considered in the design. CFD is capable of simulating flow-field at lower cost as compared with wind tunnel testing, and providing more reasonable accuracy than linear methods. Nonlinear aerodynamic optimization based on CFD becomes a key technology required to develop the next generation supersonic transport.

In order to establish advanced technologies for the next generation supersonic civil transport

(SST), Institute of Space Technology and Aeronautics of Japan Aerospace Exploration Agency (JAXA) (former National Aerospace Laboratory of Japan) has been promoting a scaled supersonic experimental airplane program, NEXST (National EXperimental Supersonic Transport) since 1997 [1]. There are two phases, un-manned non-powered (NEXST-1) and jet-powered experimental (NEXST-2) airplanes, as shown in Fig. 1 and Fig. 2, respectively. In this program, some technologies have been developed. Among these, two important technologies were developed for aerodynamic design to achieve high lift/drag ratio at supersonic cruise conditions [2]. One was an inverse method, and the other was an optimization method. Design concepts of the first airplane (Mach 2.0) included, a cranked arrow wing, a modulated warp, an area-ruled fuselage and a natural laminar flow (NLF) wing. The supersonic linear theories were applied to obtain an optimum wing and a low-drag configuration in the preliminary design. To reduce surface friction, in JAXA, an inverse method combined with CFD technology was developed to design the NLF wing, which achieves a target pressure distribution [3]. As a successor, the baseline configuration of the second airplane was designed using the same methodology of the first one. Furthermore, three approaches were adopted to improve the performance of the jet-powered experimental airplane using an inverse-optimized design system developed. 1) The inverse design method was applied to the wing design for achieving natural laminar boundary layer near the wing surface in order to reduce the friction drag. It was a challenge to conduct the inverse design method with consideration of strong integration effect between the airframe and nacelles. 2) Aerodynamic shape optimization based on CFD technology was conducted for the fuselage to design a non-axisymmetric body with a small total pressure drag and low intensity of sonic boom. 3) Nacelle shape was optimized to reduce the pressure drag and unfavorable interference between the airframe and nacelles. Details of the aerodynamic designs of the supersonic experimental airplane were described in the reference paper [2].

In the NEXST-2 program, an effective CFD-based aerodynamic design tool for complete aircraft was developed and has been applied to the jet-powered experimental airplane. It incorporates a CFD analysis code in a gradient-based optimization procedure. The major objective for using this design tool is to improve the aerodynamics performance including reduction of wave drag, induced drag, interference drag, and noise due to sonic-boom. Since 1999, the aerodynamic team of JAXA's NEXST program has applied it to the jet-powered supersonic experimental airplane. We have successfully designed the fuselage shape [4], the nacelle [5], the warp of the wing [6] [7], and a non-axisymmetric fuselage with low intensity of sonic boom [8].

This paper summarizes the CFD-based aerodynamic optimization technologies used in design of the NEXST-2 program. The methodology of aerodynamic design is described in the next section. Four design examples using the optimization tool are presented and discussed for the jet-powered supersonic experimental airplane.

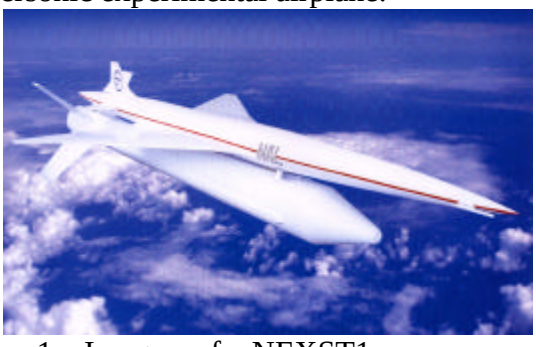

Fig. 1 Image of NEXST1: non-powered supersonic experimental airplane.

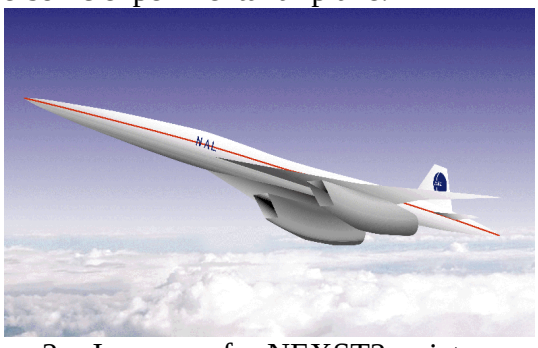

Fig. 2 Image of NEXST2: jet-powered supersonic experimental airplane.

2 Optimization Methodology of CFD-Based Aerodynamic Design

When CFD is used in the design process, the computational cost must be low enough to make the design more efficient. Main techniques of the CFD-based aerodynamic design tool are:

- A three-dimensional Euler CFD code with a multi-block/overset grid technique is used for simulating the flow-field around complex configurations. An advantage of the overset-grid technique for a CFD-based aerodynamic design is that computational grids around the corresponding component shapes can be easily re-generated for aircraft components, thus reduce computational cost.
- The gradient of the objective function is calculated using the adjoint method [4] which dramatically reduces the computation cost in each design cycle as compared with a direct finite difference method.

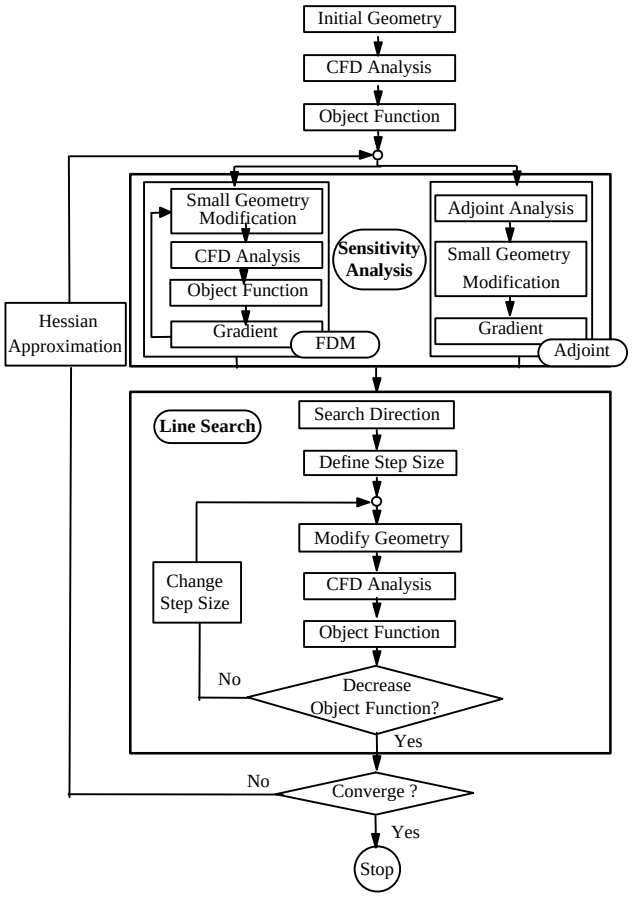

Fig. 3 CFD-based shape optimization flow chart.

2.1 Optimization Procedure

A quasi-Newton optimization technique based on a conjugate gradient method [9] is used in the optimization process. The flow chart of this design tool is shown in Fig. 3. One design cycle is composed of two processes: a gradient calculation of the objective function and minimization along the line with a direction conjugated to the calculated steepest descent direction. Starting with an initial configuration, this optimization procedure can be carried out successively to approach an optimum one.

2.2 Flow Analysis

A multi-block/overset grid technique is developed to handle the complex complete configuration. By using overset technique, grids around a component can be easily regenerated when its shape is modified. Communications among the overset grids are accomplished by interpolating the independent variables at grid boundaries. Generally at supersonic cruise condition, the pressure drag is much more sensitive to the shape variation than the surface friction drag, which is approximately proportional to the wetted area of the airplane. Therefore only the pressure drag should be considered if shape variation is small. It is reasonable to use the inviscid assumption. In JAXA's aerodynamic optimization tool, three-dimensional Euler equations are solved to estimate the objective function and analyze the flow field. A diagonalized ADI method with flux-split technique is used for implicit time integration, and Chakravarthy-Osher's TVD scheme is applied explicit convection terms.

2.3 Sensitivity Analysis

For comparison, both the finite difference method and the adjoint method are included in process of sensitivity analysis in Fig. 3. To make the computation more efficient, the gradient is calculated by solving adjoint equations, which is resulted from Euler equations according to the control theory. Detail description of adjoint equations can be found in Jameson 1995 [10] and Ruether [11]. The

adjoint method reduces the computational cost dramatically in the gradient calculation compared with that of a direct finite difference method. The benefit using the adjoint method is that the cost of computation in each design cycle is independent on the number of design variables, and is roughly equal to that of 2 or 3 flow computations. In this study, continuous adjoint equations are solved by the same methodology used for Euler equations.

2.4 Shape and Grid Modification

The B-spline function is used to modify the shape. Bezier surface patch is a special case when the number of knot is set to the number of control point. The number of grid generation is proportional to the number of design variables. For complex configurations, it is very difficult to incorporate a completely automatic process to re-generate grids, especially for multi-block structured grids. To save computational time of grid generation, a very simple algebraic method is adopted to determine the perturbation of interior grid points according to the variation of the grid points on the surface. After the surface is modified, the interior grids can be re-generated by shifting along each grid index line based on the initial grids. Furthermore, with the overset grids, this procedure is conducted only for the design component. The computational cost for grid generation in the design process is largely reduced.

3 Optimization Results of the Jet-Powered Supersonic Experimental Airplane

3.1 General Aerodynamic Design Considerations

The configuration of the jet-powered supersonic experimental airplane, namely NEXST-2, is composed of installed nacelle, diverter, wing and fuselage, as shown in Fig. 4. Flow around this configuration is strongly nonlinear and complicated by shock waves and component interferences. An Euler CFD result of the baseline configuration is shown in Fig. 5 at the design condition. In this situation, interference between elementary components, such as body, wing, nacelle and diverter were strong. Supersonic linear theories are generally no longer expected to obtain satisfactory results to reduce interference drag. Therefore, the nonlinear optimization using CFD is desirable to improve the design under consideration of engine/airframe integration effect.

Considering the cost and availability, we selected the YJ-69 by Teledyne as a candidate engine for the NEXST-2 airplane, while the wing/body configuration itself is scaled for the flight tests. The maximum diameter of the engine is even larger than that of the fuselage. To reduce the drag of the large nacelle, the upper part of nacelle was embedded in the inboard wing to reduce the wetted area and the volume. Due to the performance limitation of the selected engine and the large drag resulting from the large nacelle, we finally selected Mach 1.7 as the speed of the supersonic cruise condition.

The three-view general arrangement of the NEXST-2 airplane is shown in Fig. 4. The aspect ratio (AR) of the wing is 2.42, which is a little higher that that of the NEXST-1 airplane, in order to improve the performance at subsonic conditions. The inboard wing was designed as a subsonic leading edge with a sweep angle 66° to reduce the wave drag at the design Mach number of two, and a NACA66 digit series with 6% maximum thickness was adopted as the thickness distribution. The leading edge of the outboard wing was swept back by an angle 42° to increase the aspect ratio and thus improve the performance at subsonic and transonic conditions. Because the outboard wing had a supersonic leading edge at the design condition, a biconvex section with 3% maximum thickness was selected to reduce the profile drag. The leading edge of the inboard wing was rounded with finite radii, while the outboard wing was shaped as a sharp leading edge. The leading-edge kink was situated at about 55% station of wing semi-span from the center line. In the preliminary design, the wing was warped by Carlson's linear method to reduce lift-induced-drag at supersonic cruise conditions. Finally, the

fuselage of the baseline configuration of was area-ruled by the supersonic linear theory.

The general arrangement and aerodynamic design concepts of the NEXST-2 airplane are summarized in Fig. 4. They are: 1) a cranked arrow planform, 2) a warped wing, 3) an NLF inboard wing, 4) a nonlinear and non-axisymmetrical area-ruled body, and 5) low drag nacelles. The engine intake was designed by the propulsion system team.

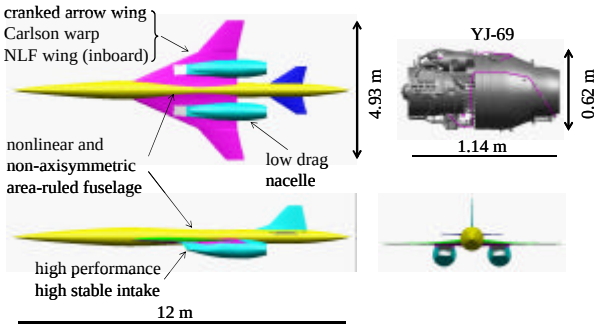

Fig. 4 Three-view general arrangement and aerodynamic design concepts of the jet-powered experimental airplane.

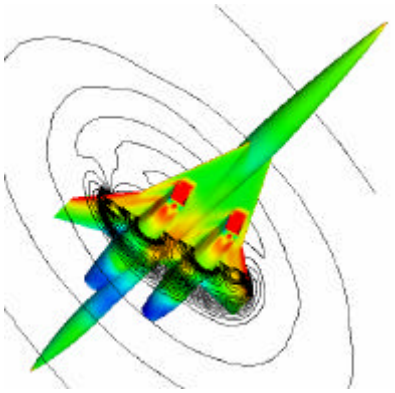

Fig. 5 Pressure distribution around the NEXST-2 airplane.

3.2 Fuselage Shape Optimization

To reduce the interference drag between components, the CFD-based optimization was applied to fuselage to replace the area-ruled one designed by the supersonic linear theory. The fuselage design is especially important for the NEXST-2 airplane due to the large nacelles, which were dominant the interference with the lower surface of the wing.

The fuselage volume of final geometry was constrained to be not smaller than a specified value V_{min}, which was the volume of the area-ruled fuselage. The objective function used in this case was defined as follows.

$$I = \frac{C_{Dp} + k\left(\dfrac{V - V_{\min}}{V_{\min}}\right)^2 H(V_{\min} - V)}{C_{Dp0}} \qquad (1)$$

The subscript 0 means the initial value. The function $H(x)$ is the Heaviside step function which replies 1 for positive value x and 0 for negative value x. The penalty coefficient k is used to satisfy the volume constraint.

The initial axisymmetrical fuselage was modified to a non-axisymmetrical one by defining separately tow ellipses with upper, lower and side radius distributions, as shown in Fig. 6. Each radius distribution is modified by the 16th Bezier curves. The total number of the design variables used in this case is $15 \times 3 = 45$. The total pressure drag is reduced 6.0 drag counts, in which 1.8 drag counts are contributed from the wing-body and 4.1 drag counts are due to two nacelle outer surfaces. In Fig. 7, geometries of the initial and optimized fuselage are compared. By optimization, the lower fuselage shape becomes different from the upper and side shape, and presents a rapid decrease of the radius at x=0.3~0.5. It seems that the increase of the equivalent area starting from x=0.4 for the nacelles, as shown in Fig. 8, is cancelled by only the lower part of the fuselage. Although the shape of the optimized non-axisymmetrical fuselage is quite different from that of the area-ruled one, the total equivalent area distribution does not deviate so much from the Sears-Haack body as compared with the axisymmetrical one. This suggests that the optimized fuselage may be one of the candidates that satisfy the area rule in the non-axisymmetrical design space. It seems that the CFD-based optimization determined a better geometry that minimized the unfavorable interference drag between the airframe and nacelles.

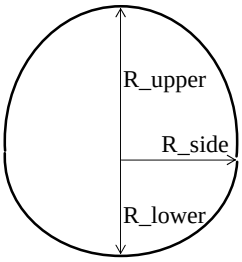

Fig. 6 Definition of the non-axisymmetrical cross section of the fuselage.

(a) initial shape of the fuselage

(b) optimized shape of the fuselage

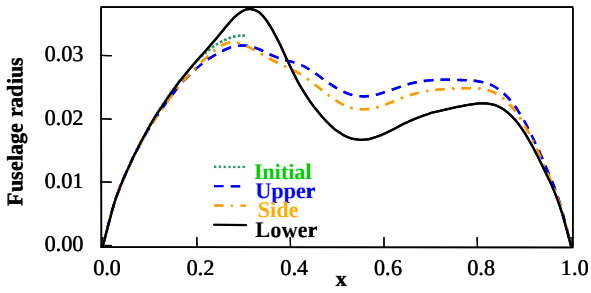

(c) radii distributions of the fuselage

Fig. 7 Comparison of the linearly area-ruled and optimized fuselages.

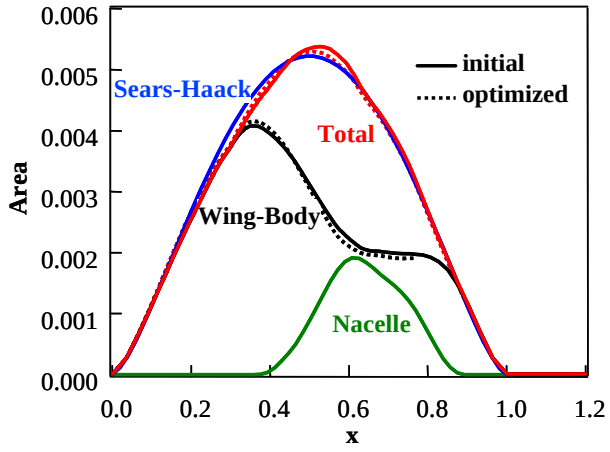

Fig. 8 Equivalent area distributions of the linearly area-ruled and non-axisymmetrical optimized fuselages.

3.3 Nacelle Shape Optimization

The developed design tool is applied to the shape optimization of an engine nacelle which is installed in the jet-powered experimental airplane (NEXST-2) at supersonic flight condition of Mach 1.7 and angle-of-attack α=0.5deg to minimize the total airplane drag. In this situation, the installation effect is significant. One of the objectives of this research is to find an effective design concept for an SST aft-nacelle geometry to reduce the wave drag with the consideration of airframe/nacelle and nacelle/nacelle interference. The fore-nacelle had to be fixed because of design constraints of the propulsion system. Therefore, the design region was selected as the aft-nacelle, as shown in Fig. 9. Geometric constraints of G^2 continuities are imposed on the boundaries of the design domain. To modify the nacelle shape, we use 2D Bezier patch with 8 control points in the axial direction and 7 control points in the circumferential direction. The number of grid points is about 1.65 million, and the computational grid system is composed of 2 blocks for the major grids around the wing/fuselage and 4 blocks for the minor grids around the nacelle/diverter. The design is converged in about 20 design cycles and the pressure drag is reduced by 5.7 drag counts. Compared with that of the aft-nacelle surface of the baseline configuration in Fig. 10, an expansion region of the optimum nacelle propagates down more rapidly and therefore the pressure is recovered earlier. It is shown that the optimization tries to make the slope of the aft-nacelle as small as possible. Probably, this conclusion can be extended to modify the diverter. According to this observation, the aft-nacelle shape as well as the diverter is re-defined using a CAD software. As a result, this action successfully reduced the pressure drag by 9.8 counts. The baseline, optimum and final CAD definition of the aft-nacelle geometry are compared in Fig. 10. This design result indicates that a conical frustum type aft-nacelle shape minimizes the pressure drag for a given nacelle length and maximum diameter.

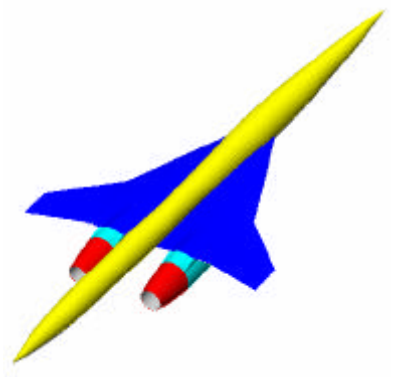

Fig.9 Aft-nacelle design region.

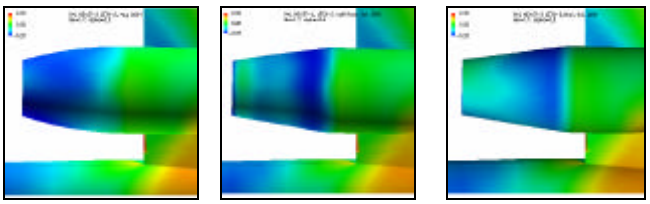

(a) initial (b) optimized (c) CATIA final

Fig. 10 Aft-nacelle shape optimization result and final CATIA shape definition.

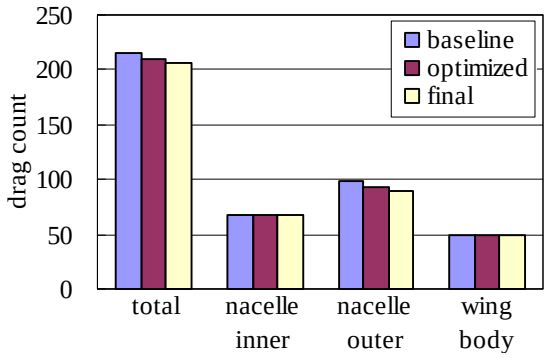

Fig. 11 Comparison of pressure drag.

3.4 Wing Warp Optimization

This is a fundamental research and it is not reflected in the final design of the NEXST-2 airplane. According to the Prandtl linear wing theory, the lift induced drag is only dependent on the lift distribution, and minimum induced drag occurs when the lift is distributed in an elliptic fashion. So, one of the best ways to reduce the induced drag is to change the twist and camber distributions by an optimum lift load distribution, thus achieve a minimum drag. Conventionally, the linear method of supersonic lifting surface theory has been used in the warp design. The linear method may be used as an interactive manner which is not possible with more sophisticated CFD methods. In the preliminary design phase, it works very efficiently to predict the aerodynamic performance efficiently and is easy to be implemented with design concepts. However, the linear method of warp design does not include nonlinear effects, such as thickness distribution, volume, component interference, and so on. By contrast, CFD does not have such restrictions. Furthermore, the CFD-based optimization method can produce possible designs in wider design space than the linear method.

The objective of this research is to reduce pressure drag and improve the load distribution by modifying the twist distribution and the camber surface. Warp optimization of the wing was conducted to optimize the twist and camber surface of the wing/body configuration at supersonic cruise condition. Fig. 12 shows the method to modify the shape of the wing section using a Bezier curve. The objective function is defined as follows.

$$I = \frac{C_{Dp}}{C_{Dp0}} + k\left(\frac{C_{Lp} - C_{Lp0}}{C_{Lp0}}\right)^2 \qquad (2)$$

The lift is fixed and the pressure drag is forced to reduce in the optimization design.

Pressure distributions are shown in Fig. 13. The initial thickness distribution was designed by the inverse method. As shown in the pressure distribution at 30% wingspan, the strong expansion waves, which were generated by the convergent part of the fuselage, interfered with the upper surface of the wing and may result drag penalty. By optimization, the camber became larger and reduced the expansion waves on the upper surface. The optimization made the pressure distribution change significantly at the outboard in Fig. 13(b).

Load distributions of the baseline and optimized shapes in the spanwise direction are compared in Fig. 14. Because the intersection of the wing and the fuselage was fixed in optimization design process, the section lift and

drag near the intersection were almost not changed. Compared with that of the baseline shape, the optimized lift load is improved and is closer to an elliptic distribution as shown in Fig. 14(a). It shows that the drag reduction has mainly taken place within the inboard wing of 30% wingspan from the body axis. On the outboard wing, although the pressure drag was almost not changed, the lift distribution was significantly reduced. The optimization moves the lift distribution inboard, and produces smaller wing bending stresses.

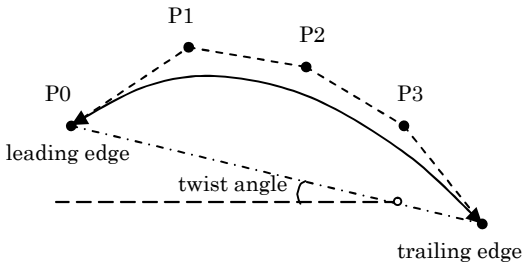

Fig. 12 Camber and twist defined by Bezier function.

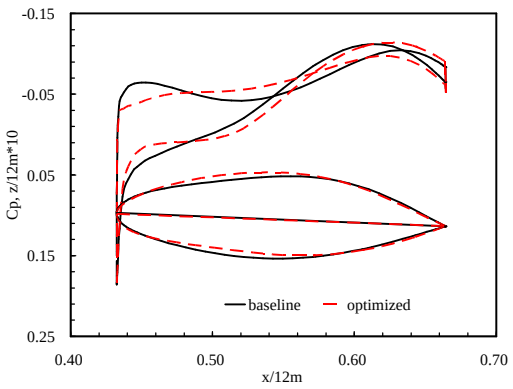

(a) y=0.3 semi-span.

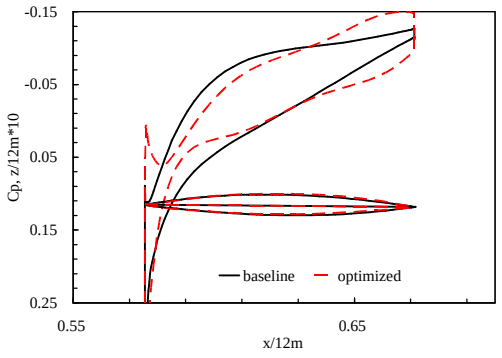

(b) y=0.7 semi-span.

Fig. 13. Initial and designed shapes and pressure distributions.

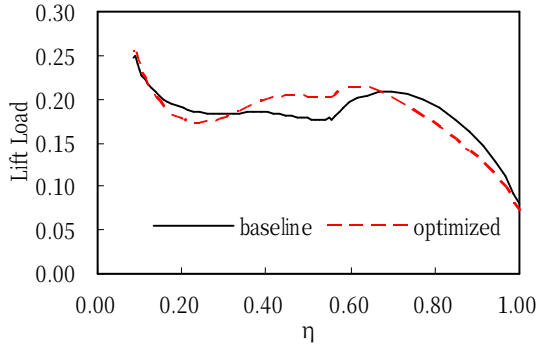

(a) lift

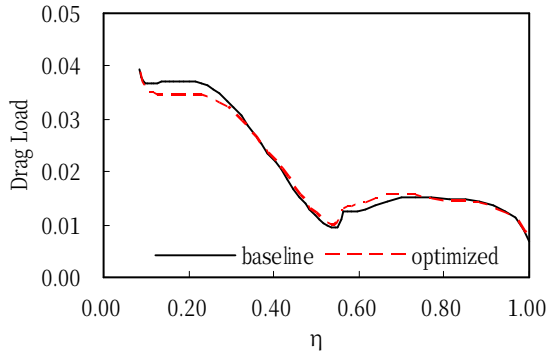

(b) drag

Fig. 14: Load distributions on the wing in the spanwise direction.

3.5 Low-Boom / Low-drag Fuselage Optimization

One of the most important technologies for the next generation supersonic transport is the design of reducing the sonic boom caused by supersonic overland flight. The sonic boom should be reduced as low as possible to make the flight environmentally feasible. Thus, the low sonic-boom design of the experimental airplane with jet engines is studied as a design option the NEXST-2 program. Although conventional methods have found some solutions with low sonic boom, their area distribution with blunt nose shape also produced large drag. A trade-off between airplane drag and sonic-boom intensity is needed. The upper and lower surfaces of the fuselage place different roles in the design. Because the former dominates the sonic boom propagated to the ground, it is naturally thought to be effective for low-boom design. On the other hand, the later

does not contribute so much relatively, and it may be designed for the drag reduction. It is suggested that they may be designed separately with different objectives. Therefore, the non-axisymmetrical fuselage design described in the previous section also has large potential to find a low sonic-boom configuration with minimum drag penalty. This low-drag/low-boom design method is applied to a configuration with fuselage, main and tail wings.

The baseline shape, so called low-drag configuration in this section, was designed for drag reduction with the Sears-Haack area distribution. For comparison, the baseline fuselage was replaced by a low sonic-boom designed one, which was called low-boom configuration here. Both of the fuselages of the low-drag and low-boom configurations are axisymmetrical. The optimized shape of the low-drag/low-boom configuration is shown in Fig. 15. In the near field in Fig. 16(a), two shocks from the nose and wing are clearly seen under the low-drag airplane. On the other hand, pressure signatures for the low-boom and low-drag/low-boom configurations show flat-top like shapes in the front part and the peaks due to the wing shock are much lower than that for the low-drag one. To predict a sonic-boom pressure signature, these near-field pressure signatures are extrapolated to the ground by the waveform parameter method at flight conditions of Mach number 1.7 and attitude 15 km. Fig. 16(b) shows the extrapolated ground pressure signatures for these three configurations. The ground signature for the low-drag configuration is typical “N-shaped” signature whose initial pressure rise is about 0.47psf and duration time is about 53ms. On the other hand, the signatures for the other two configurations still keep non-N-shaped signatures on the ground and the initial peak pressure levels are about 0.15psf smaller than that for the low-drag configuration. Fig. 17(a) and (b) show the aerodynamic properties for the configurations estimated by the CFD analyses. The slope of CL-α curve is slightly reduced by the axisymmetrical low sonic-boom design. The CL-α curve shifts downward by the non-axisymmetrical design. The polar curve (CDp-CL curve) shifts upward by the axisymmetrical low sonic-boom design from the curve for the low-drag configuration. The polar curve for the low-drag/low-boom configuration locates between the two curves. The drag of the low-boom configuration is 96 drag counts which is 20 counts larger than that of the low-drag configuration. The non-axisymmetrical fuselage design reduces the pressure drag of the low-boom configuration about 12 counts without increasing its sonic-boom intensity. The results show efficiency of the non-axisymmetrical fuselage design for reducing pressure drag of the low-drag/low-boom airplane although the pressure drag of the low-drag/low-boom configuration is still larger than that of the low-drag configuration about 8 counts.

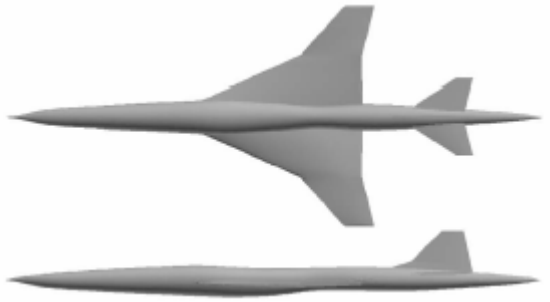

Fig. 15 Low-drag/low-boom configuration

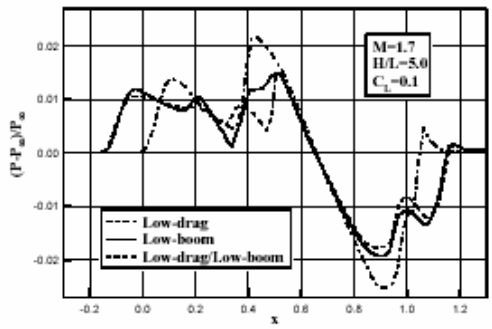

(a) CFD-predicted near field

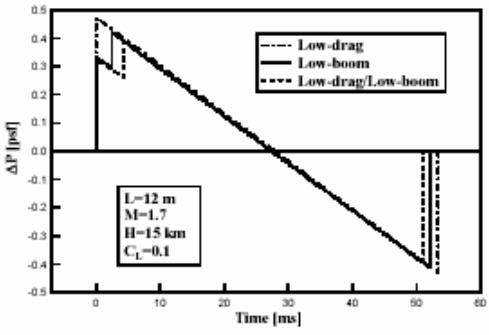

(b) extrapolation of the ground

Fig. 16 Pressure signatures

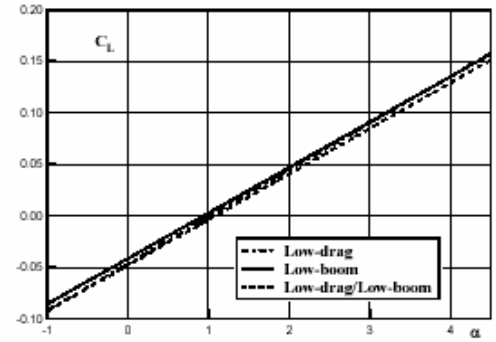

(a) CL-α curves

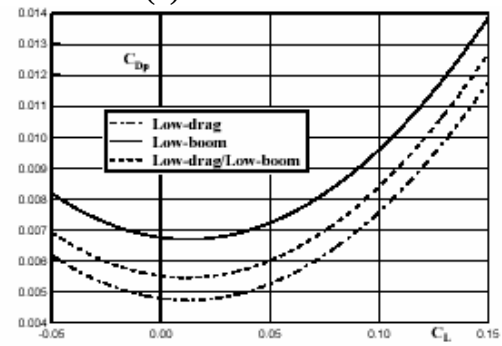

(b) polar curves

Fig. 17 Aerodynamic properties

Conclusions

An aerodynamic design tool which incorporates a three-dimensional Euler CFD code in a gradient-based optimization procedure was developed in the Japanese supersonic experimental transport program. It is featured by a three-dimensional Euler CFD analysis with a multi-block/overset grid technique and an adjoint sensitivity analysis derived from control theory. During the latest few years, this computational design tool has been applied to the aerodynamic shape designs of the jet-powered supersonic experimental airplane. It shows that this computational tool is capable of improving aerodynamic performance of aircraft. CFD-based optimization techniques have been proven to be efficient in the aerodynamic shape design for complex configuration, largely shorten the overall design process and reduce cost.

Acknowledgement

The authors would like to acknowledge the contribution and the help of the staff of the aerodynamic team of JAXA's supersonic experimental transport program.

References

[1] Sakata K, Supersonic research program in NAL, Japan, *1st International CFD Workshop for Super-Sonic Transport Design*, Tokyo, pp.1-4, 1998.

[2] Yoshida K and Makino Y. Aerodynamic design of unmanned and scaled experimental airplane in Japan. *ECCOMAS 2004*, Jyväskylä.

[3] Matsushima K, Iwamiya T, Jeong S and Obayashi S. Aerodynamic wing design for NAL's SST using iterative inverse approach, *1st International CFD Workshop for Super-Sonic Transport Design*, Tokyo, pp.73-78, 1998.

[4] Makino Y, Iwamiya T and Lei Z. Fuselage shape optimization of a wing-body configuration with nacelles, *Journal of Aircraft* Vol.40, No.2, March-April 2003, pp297-302.

[5] Lei Z, Makino Y. and Iwamiya T. Nacelle design study of a supersonic experimental airplane using aerodynamic shape optimization, *40th Aerospace Sciences Meeting & Exhibit*, AIAA paper 2002-0105, Reno, NV, Jan. 2002.

[6] Lei Z and Makino Y. CFD-based warp optimization for the wing of a supersonic experimental airplane using adjoint method, (in Japanese), *Proceedings of 40th Aircraft Symposium*. Oct. 2002, Yokohama, Japan.

[7] Lei Z, Makino Y and Yoshida K. Warp design of a supersonic wing using a nonlinear optimization method, *42nd Aerospace Sciences Meeting & Exhibit*, AIAA paper 2004-0216, Reno, NV, Jan. 2004.

[8] Makino Y, Suzuki K, Noguchi M and Yoshida M. Nonaxisymmetrical fuselage shape modification for drag reduction of a low sonic-boom airplane. *AIAA Journal*, Vol.41, No.8, pp.1413-1420, 2003.

[9] Press W, Teukoisky S, Vetterling W and Flannery B. *Numerical Recipes in FORTRAN*, Second Edition, Cambridge University Press, pp.418-423.

[10] Jameson A. Optimum aerodynamic design using CFD and control theory, *AIAA paper* 95-1729, 1995.

[11] Reuther J. *Aerodynamic Shape Optimization Using Control Theory*, Ph.D. Dissertation, Univ. of California, Davis, CA, June, 1996.